Muscle forces and spinal loads at C4/5 level during isometric voluntary efforts

HYEONKI CHOI and RAY VANDERBY, JR.

Division of Orthopedic Surgery and Department of Mechanical Engineering, University of Wisconsin-Madison, Madison, WI

ABSTRACT

CHOI, H. and RAY VANDERBY, JR. Muscle forces and spinal loads at C4/5 level during isometric voluntary efforts. Med. Sci. Sports Exerc., Vol. 32, No. 4, pp. 830-838, 2000. Purpose: The goal of this study was to determine neck muscle forces and spinal loads that result from isometric muscle contractions. Methods: Electromyographic (EMG) activity of the neck musculature and a threedimensional biomechanical model of the neck were used. The model was EMG-based and estimated muscle forces and spinal loads at the C4/5 level. EMG signals were collected from eight sites at the C4/5 level of the neck using Ag-AgCl surface electrodes from 10 adult male subjects. The subjects performed isometric contractions gradually developing to maximum efforts in flexion, extension, left lateral bending, and right lateral bending. Results: During maximum voluntary contraction (MVC) trials most muscles generated high levels of EMG signal during cervical rotation. The posterior surface of the neck (trapezius) was the only electrode site at which maximum activity EMG consistently occurred by the same method (rotation) in all subjects. Variations in the EMG patterns were observed in different experiments that produced overall neck moments of equal magnitudes. With these data the model computed variations in load distribution among the agonist muscles. Consistent also with EMG distributions, the model also computed co-contractions of antagonist muscles. The average (± SD) magnitudes of peak moments were 28.3 (± 3.3) Nm in extension, 17.7 (± 3.1) Nm in flexion, 16.9 (± 2.8) Nm in left lateral bending, and 17.0 (± 2.9) Nm in right lateral bending. The model predicted C4/5 joint compressive forces during peak moments were 1372 (± 140) N in extension, 1654 (± 308) N in flexion, 956 (± 169) N in left lateral bending, and 1065 (± 207) N in right lateral bending. Conclusions: Results suggest that higher C4/5 joint loads than previously reported are possible during maximum isometric muscle contractions. Key Words: CERVICAL SPINE, NECK MODEL, MAXIMUM VOLUNTARY CONTRACTION, ANTAGONISTIC CO-CONTRACTION

njury of the cervical spine presents a number of diagnostic issues with frequent sites of cervical spinal injury at the C5 level (74%), C4 level (16%), and C6 level (10%) (27). The pathogenesis of neck pain, however, is often unknown (24). Generally, mechanical factors are involved in the cause of some neck pain. Thus, a better knowledge of the neck muscle forces and spinal loads imposed by the performance of physical tasks will help differentiate possible causes of neck pain. In addition, this knowledge will be useful for diagnostic, surgical, preventive, and rehabilitative medicine.

One of two possible approaches, the optimization technique or the EMG-based technique, is typically used to solve the statically indeterminate problem in biomechanical modeling of body segments. Although optimization models have proven useful in predicting muscle forces from intersegmental moments, some discrepancies between model predictions and empirical results exist. For example, some coefficients of linear correlation between predictions of a neck model and experimental results were 0.29 and 0.33

(16). A major weakness of optimization models is that they do not predict co-contraction of antagonistic muscles, yet the co-contraction of muscles developing opposing moments about a joint is a common experimental observation (11). The optimization models often predict muscles to be inactive in situations where significant EMG activity is observed (9,19,21,22).

The EMG-based approach, on the other hand, predicts co-contractions of antagonistic muscles together with the various patterns of agonistic synergy (13). The EMG-based approach is sensitive to subject and trial differences in the magnitudes of individual muscle forces needed to produce the same reaction moment. In contrast, the optimization method shows a similar estimate of muscle forces for all subjects and trials producing the same moment. The EMG-based model has proven to be a valuable method to determine muscle forces and spinal loads in the low back. For example, a dynamic model of the lumbar spine was used to estimate forces in active tissues using a myoelectrically based strategy and in passive structures from estimates of strain (12–14).

Several studies have investigated the effects of co-contraction with lumbar models. To evaluate the effects of co-contraction, Hughes et al. (8) applied K-K-T (Karush-Kuhn-Tucker) multipliers to a human lumbar optimization model. Their results showed that spinal compression can be

0195-9131/00/3203-0830/0 MEDICINE & SCIENCE IN SPORTS & EXERCISE $_{\tiny\textcircled{\tiny{1}}}$ Copyright © 2000 by the American College of Sports Medicine

Submitted for publication March 1998. Accepted for publication June 1999.

increased substantially by co-contraction and that, in special circumstances, co-contraction may be able to decrease the spinal compression in a conventional torso optimization model that is used extensively in studies of the lumbar spine. Cholewicki et al. (3) myoelectrically examined antagonistic muscle co-contraction during slow trunk flexion and extension tasks around neutral posture. When mechanical stability criteria were considered, their inverted pendulum trunk model predicted trunk muscle co-contraction levels necessary to maintain spine stability that corresponded very well to their experimental results. In addition, they observed that antagonistic muscle co-contraction increased in response to increased axial load on the spine. Thelen et al. (26) used a myoelectric signal-muscle stress model and consecutive optimization routines to calculate muscle forces including cocontraction in a human lumbar spine model. To quantify the degree of co-contraction, they subdivided the predicted muscle forces into two sets, task-moment set and co-contraction set of muscle forces that produced zero net moment. Their analysis suggested that substantial contractions of lumbar muscles, especially during asymmetric exertions, are used for reasons other than equilibrating moments at the L3-L4 level.

To our knowledge, there have been no biomechanical models of the neck that have used an EMG-based approach and therefore no models that have considered the effects of antagonistic muscle forces on cervical spinal loading. Pursuant to these effects, the following hypotheses were tested in this study: 1) substantial levels of antagonistic co-contractions and variations in muscle activation are present in neck musculature of neutral posture during voluntary isometric efforts; 2) the EMG-based model predicts various muscle force distributions including antagonistic muscle forces that correspond to the cervical muscle activation patterns; 3) when including antagonistic muscle forces in an EMG-based model, estimates of spinal compressive loads are higher than previously reported.

METHODS

Experimental design. Ten healthy male volunteer subjects (mean age \pm SD: 31.2 ± 2.0 yr) who had no history of neck injury or notable neck pain participated in the experiment. Each subject provided written informed consent to participate. The experimental protocol was approved by the Department of Kinesiology Human Subjects Committee, University of Wisconsin-Madison. The subjects were asked to sit in a chair. Their upper body and arms were strapped with Velcro (Velcro USA, Manchester, NH) to a board fixed behind the chair and their hands placed on their laps. A headband (made with Velcro) was worn by each subject, and the headband was connected with a rope to a fixed force transducer.

Electromyographic signals were measured with eight pairs of bipolar Ag-AgCl surface electrodes (diameter of disk, 6 mm; Grass Instruments, Quincy, MA) affixed around the neck at the C4/5 level. The C4/5 level was located by palpation of the vertebrae. Eight electrode locations were

bilaterally denoted as anterior, anterolateral, posterolateral, and posterior. Their locations approximated azimuth angles of 35°, 70°, 105°, and 150°, respectively: midway between the anterior midline and the anterior border of the sternocleidomastoid (SCM) muscle, midway between the anterior and posterior borders of the SCM muscle, midway between the posterior border of the SCM muscle and anterior border of the upper trapezius muscle, and midway between the anterior border of the upper trapezius muscle and the posterior midline (16). In this study all metal disk poles within a pair of bipolar surface electrodes were spaced between 10 and 20 mm apart center to center.

After the electrodes were affixed, each subject performed two sets of isometric tasks calling for neck muscle contractions. The first set of tasks was to provide a basis for EMG normalization. It consisted of maximum isometric efforts to produce the largest amplitudes of EMG activity from the selected neck muscles. For this purpose two basic isometric restraint strategies were used in which subjects attempted to produce maximum muscle activity. The first strategy consisted of maximum isometric exertions while the subject was sitting on a restraint chair. The upper body was fixed to the chair, and the head was restrained by a cord and head strap from a fixed wall. Then extension, flexion, left lateral bending, and right lateral bending efforts were performed with resistance supplied by the wall. The second strategy was to record muscle activity during maximum isometric rotation efforts. These rotation efforts were performed with the head in neutral position, 30° prerotated to the left, and 30° prerotated to the right with the body and neck in an upright posture. An assistant provided a matching resistance to the subject's head during the maximum rotation effort. During the first set, loads were measured for extension, flexion, lateral bendings, but rotation loads were not measured. Three trials were collected during the first set. The largest EMG activity observed during any of these strategies was taken as 100% MVC for each particular muscle.

In the second set of tasks, subjects performed near maximum, isometric, and voluntary efforts in extension, flexion, left lateral bending, and right lateral bending. Each subject was instructed to gradually build up to maximum efforts, peaking at about 5 s. Three trials of each effort were performed. During the second set, all loads were measured by a fixed force transducer. In total, each subject performed 42 isometric quasi-static tasks. A 2-min recovery period was allowed between contractions to avoid fatigue.

The EMG signals were preamplified, further amplified, full-wave rectified, low pass filtered (cutoff frequency: 3 Hz) (using Grass Instruments), and A/D converted (100 Hz) sequentially. Finally, the digitized signals were saved to a personal computer. Signals from the force transducer were fed to an amplifier, A/D converter (100 Hz), and then saved to the computer.

Measured external loads and the estimated weights of the subjects' heads were used as input values of the model. The weight of the head was assumed to be 7.3% of the subject's total body weight with a center of mass acting midway between the ears (5).

TABLE 1. Grouping of muscles modeled on each side of the neck

	Muscles Grouped
Anterior	Platysma, infrahyoid
Anterolateral	Sternocleidomastoid, longus colli and cervicis, scalene anterior
Posterolateral	Scalene medius, longissimus cervicis, levator scapulae, slpenius cervicis
Posterior	Multifidus, semispinalis cervicis, semispinalis capitis, slpenius capitis, trapezius

EMG-based biomechanical neck model. To construct the human neck model, the origin of an orthogonal coordinate system was located at the disk center of the C4/5 level. Positive directions were chosen as the left, posterior, and superior. In this model the C4/5 motion segment was assumed to resist only compressive and shear forces but not bending or rotational moments (16). This assumption was also used with lumbar spine motion segments by Schultz et al. (19-21). In this study we used anatomical data of the neck model reported by Moroney et al. (16). They used a scaled cross-sectional anatomy drawing of the C4 level to calculate the anatomical data. To determine the relative area of the cross-section of each muscle, they pasted a reproduction of the drawing onto a uniform sheet of cardboard and then weighed cutouts of each muscle cross-section and the total cross-section defined by the neck diameters. They used linear scaling to determine the centroid locations relative to neck diameters and used scaled cross-sectional drawings at adjacent levels to determine the muscle lines of action. Muscle centroidal coordinates were expressed relative to the frontal and sagittal plane neck diameters; their areas were scaled relative to the product of the diameters.

In this study, 14 pairs of muscles (28 muscles) were modeled and grouped to correspond to eight electrode sites. For example, left platysma and left infrahyoid consist of one group at the left anterior position. The grouping of the muscles (Table 1) is based on the assumption that muscles in the same group experience the same EMG activities as a percent of MVC.

Muscle forces were assumed to have a power relationship with the mean rectified EMG signal expressed as a fraction of maximum EMG activation level based on the data of Stokes et al. (25) and Vink et al. (29). Cholewicki et al. (4) also supported this nonlinear relationship from their experiment.

$$f_i = \left(\frac{emg}{emg_{max}}\right)^{1/1.3} a_i \sigma_{max} \tag{1}$$

where f_i is the *ith* muscle force (N); a_i is the *ith* muscle cross-sectional area; σ_{max} is the maximum muscle force generated per unit of cross-sectional area (3.5 × 10⁵ N/m²); emg/emg_{max} is the muscle activation level expressed as a fraction of its maximum EMG activity (2). The passive force was neglected for this isometric experiment.

A common gain for all muscle EMG signals was calculated by using a least square method fitting the model predictions and measured moments.

$$M_{emg_x} = \sum_{i=1}^{n} (r_{yi}f_{zi} - r_{zi}f_{yi}), n = 28$$

$$M_{emg_y} = \sum_{i=1}^{n} (r_{zi}f_{xi} - r_{xi}f_{zi}), n = 28$$
 (2)

$$M_{emg_{z}} = \sum_{i=1}^{n} (r_{xi}f_{yi} - r_{yi}f_{xi}), n = 28$$

$$\sum_{k=x,y,z} (GM_{emg_{k}} - M_{k})^{2} = min$$
(3)

where M_x , M_y , and M_z are total moments necessary to balance moments acting on the joint about x, y, and z axes; G is common gain; f_{xi} , f_{yi} , and f_{zi} are estimated individual muscle forces in the x, y, and z joint axes directions, respectively; r_{xi} , r_{yi} , and r_{zi} are muscle moment arms with respect to the x, y, and z joint axes; and $M_{emg_{x,y,z}}$ is the total moment calculated from muscle forces acting on the joint about x, y, and z axes (2). A common gain, G, is introduced to compensate for overall systematic errors in the initial assessment of muscle forces (4).

For calculation of the EMG-based model, each EMG signal was normalized to the maximum EMG value obtained from the MVC trials. Then, with these normalized EMG values and EMG-muscle force relationship (equation 1), the first assignment of muscle forces was made. These steps were done on a spread sheet (Quattro Pro 6.0, Novell, Inc., Orem, UT). The gain value, G, was calculated using MATLAB (MATLAB V4.2c0.1, The MathWorks, Inc., Natick, MA) with EMG-based model program and the first muscle forces assignment. After the gain value was obtained, the final muscle forces were calculated by multiplying the first muscle forces set by the gain value. With these final muscle forces, the spinal loads were also calculated with MATLAB.

To test the accuracy of the model predictions, root mean square (RMS) errors of the model predicted moments were calculated. The RMS error is defined as

RMS error =
$$\sqrt{\frac{1}{n} \sum_{i=1}^{n} \left(\frac{M_{emg} - M_{meas}}{M_{meas}}\right)^2}$$
 (4)

where n is the number of trials, M_{meas} is the measured external moments, M_{emg} is the model predicted external moments. If the measured external moments are identical to model predicted moments, the RMS error is equal to zero. Any nonzero value of the RMS error indicates the difference between measured external moments and model-predicted moments.

TABLE 2. Methods that produced the maximum EMG activity at each muscle equivalent

Muscle Equivalent	Number of Subjects and Method			
L platysma	6 flex, 2 twist 0° cw, 1 twist 30° cw, 1 twist 0° ccw			
R platysma	6 flex, 3 twist 0° ccw, 1 twist 0° cw			
L sternocleidomastoid	4 twist 0° cw, 3 twist 30° cw, 3 flex			
R sternocleidomastoid	4 twist 0° ccw, 3 twist -30° cw, 2 flex, 1 right bend			
L levator scapulae	2 twist -30° cw, 2 twist 0° ccw, 1 twist 0° cw, 1 twist 30° cw, 1 twist 30° ccw, 1 exten, 1 flex, 1 left bend, 1 flex, 1 left bend			
R levator scapulae	4 right bend, 2 twist 0° cw, 1 twist 30° cw, 1 twist 30° cw, 1 twist -30° ccw, 1 exten			
L trapezius	7 twist 30° ccw, 3 twist 0° ccw			
R trapezius	6 twist 30° cw, 4 twist 0° cw			

RESULTS

Maximum voluntary contractions (MVC) and **EMG activities.** The methods that produced maximum muscle activities for each electrode location are shown in Table 2. The trapezius was the only electrode location in which maximum activity consistently occurred with the same method (rotation) in all subjects. Left trapezius occurred with rotation in counter-clockwise (ccw) direction and right trapezius with rotation in clockwise (cw) direction, whereas EMG activity was greatest in platysma with flexion and in SCM with rotation and flexion. For the levator scapulae there was not a dominant method for obtaining the maximum EMG activity consistently. The mean (± SD) EMG activities expressed as a percent of MVC during isometric peak exertions are shown in Table 3. It is noteworthy that the rotation mode proved to be an excellent method for obtaining the maximum EMG activities for all of the neck muscles. The mean (\pm SD) EMG activities of each neck muscle during peak isometric rotation were 91.0 (± 12.0) % MVC in trapezius, 77.6 (± 18.5) % MVC in SCM, 77.3 (± 19.9) % MVC in platysma, and 66.4 (± 21.2) % MVC in levator scapulae.

During rotation mode, the relative EMG activity within a given muscle appears to be associated more with direction of rotation than the angle at which rotation started. Bilaterally in the trapezius, it appears that the starting position of rotation affects the relative EMG level. A $+30^{\circ}$ prerotated starting position tends to increase the EMG level, and -30° prerotated starting position tends to decrease the EMG level in each respective direction of rotation.

The relationships of external moments versus EMG (% MVC) (Figs. 1 through 3) were not consistently linear among subjects or between trials of subjects. Although EMG signal amplitude generally increased with an increase in moment, the ramp loading did not always result in a smooth progression of the EMG activity. In flexion, agonistic muscles (platysma and sternocleidomastoid) showed a consistent linear behavior across the subjects and trials (Fig. 2). The external moment versus EMG (% MVC) graph shows how the EMG signal developed in the antagonistic muscles. At near maximal moments, co-contraction increased significantly. Compared with the other efforts, lateral bending produced the highest EMG signal level in the antagonistic muscles (Fig. 3).

There were consistent trends of phasic relationships in muscle recruiting patterns. In extension, the trapezius becomes active earlier than levator scapulae. Levator scapulae showed a precipitous increase in activity from about three-quarters of the whole ramp period. In flexion the agonists (platysma, SCM) showed similar phasic patterns. These agonist muscles become active early and remained active throughout the whole ramp period. In lateral bending, all the muscles (agonists, antagonists) became active in the exertions.

Measured and model calculated moments during peak efforts. The mean (± SD) voluntary peak external moments developed by the 10 subjects were 28.3 (± 3.3) Nm in extension, 17.7 (\pm 3.1) Nm in flexion, 16.9 (\pm 2.8) Nm in left lateral bending, and 17.0 (\pm 2.9) Nm in right lateral bending. The mean (± SD) model-predicted peak moments about lateral, anteroposterior, and axial axes were, respectively: 30.2 (\pm 5.7) Nm, 0.7 (\pm 0.4) Nm, and 0.3 (\pm 0.2) Nm during extension; 15.6 (\pm 5.1) Nm, 1.5 (\pm 0.7) Nm, and 0.3 (\pm 0.2) Nm during flexion; 6.2 (\pm 2.9) Nm, 13.2 (\pm 6.5) Nm, and 3.2 (\pm 1.8) Nm during left lateral bending; 6.1 (\pm 3.5) Nm, 12.4 (\pm 5.8) Nm, and 2.4 (\pm 1.4) Nm during right lateral bending. The RMS errors of the model-predicted moments about each corresponding axis were 0.07 in extension, 0.12 in flexion, 0.23 in left lateral bending, and 0.28 in right lateral bending.

Model calculated muscle forces and spinal loads. Table 4 shows the mean (across subjects) muscle forces predicted during peak moments. Mean (± SD) calculated neck muscle contraction forces ranged up to 302 (± 89) N. The maximum muscle force occurred in the SCM during peak flexion exertions. Figures 4 through 6 show the distribution of muscle forces, including antagonistic cocontractions predicted by the model. The antagonists consist of the anterior neck muscles in extension, the posterior neck muscles in flexion, and right side muscles in left lateral bending. The model simulated the maximal co-contraction of antagonist muscles in the vicinity of a peak moment as was seen from EMG behaviors expressed as a percent of MVC. The model simulated the various load distribution patterns among the agonist muscles during the generation of moments of equal magnitudes, especially in lateral bending. These variations existed not only between the subjects but also between trials of the same subject (Fig. 7).

 ${\small TABLE~3.~Mean~EMG~activity~expressed~as~a~\%~MVC~during~isometric~peak~efforts~with~SD~in~parentheses.}$

Isometric Effort	Left Platysma	Right Platysma	Left SCM	Right SCM	Left Levator scap.	Right Levator scap.	Left Trapezius	Right Trapezius
Extension	3.1 (2.2)	2.3 (1.7)	3.4 (2.0)	4.9 (2.8)	47.9 (22.2)	54.9 (20.8)	50.9 (19.7)	47.1 (21.9)
Flexion	83.2 (13.4)	84.7 (10.6)	70.9 (19.9)	77.9 (15.5)	23.2 (15.5)	28.4 (18.1)	6.1 (3.6)	5.5 (4.8)
L lat. bend	53.4 (19.1)	25.6 (17.2)	56.3 (14.0)	15.4 (14.7)	63.3 (34.5)	10.4 (8.6)	33.9 (17.9)	9.9 (12.3)
R lat. bend	43.9 (19.7)	60.6 (18.0)	21.4 (14.8)	65.7 (19.0)	5.1 (3.0)	58.6 (19.2)	10.3 (5.1)	37.5 (19.9)
0° cw	77.3 (19.9)	62.4 (30.6)	75.9 (17.0)	52.9 (24.2)	63.0 (30.7)	54.6 (24.1)	50.5 (14.6)	83.1 (11.1)
+30° cw	72.8 (21.1)	58.5 (24.0)	77.6 (18.5)	49.1 (18.8)	59.2 (31.5)	58.2 (29.6)	58.6 (20.5)	91.0 (12.0)
-30° cw	66.0 (17.0)	64.8 (18.7)	66.8 (17.3)	58.4 (24.4)	62.6 (16.3)	60.3 (12.1)	54.2 (20.7)	70.8 (11.7)
0° ccw	51.7 (31.2)	75.5 (16.8)	49.9 (29.0)	73.5 (22.3)	57.5 (20.6)	53.6 (13.1)	76.5 (17.1)	47.9 (18.7)
+30° ccw	44.8 (26.8)	64.7 (18.3)	44.7 (20.8)	66.6 (26.1)	59.3 (19.5)	66.4 (21.2)	83.0 (18.8)	50.2 (19.6)
-30° ccw	58.0 (21.9)	60.2 (10.6)	55.6 (22.7)	59.4 (11.9)	52.6 (28.1)	57.7 (27.8)	74.0 (14.2)	45.1 (14.0)

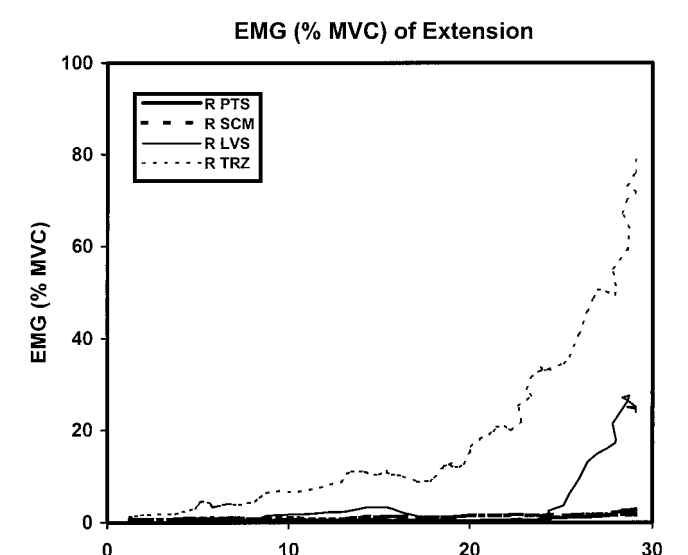


Figure 1—External moments—EMG (% MVC) relationship developed in attempted extension (right side: subject 5). R PTS, right platysma; R SCM, right sternocleidomastoid; R LVS, right levator scapulae; R TRZ, right trapezius.

External moment (Nm)

Samples of each normalized EMG signal were selected for input into the model. Mean spinal loads during peak attempted efforts (lateral shear, anteroposterior shear, compressive force) are shown in Table 5. The mean (\pm SD) C4/5 joint compressive forces predicted during peak moments were 1372 (\pm 140) N in extension, 1654 (\pm 308) N in flexion, 956 (\pm 169) N in left lateral bending, and 1065 (\pm 207) N in right lateral bending. The maximum mean (\pm SD) shear forces predicted during peak moments were 182 (\pm 28) N in lateral direction and 89 (\pm 39) N in anteroposterior direction. The maximum lateral shear forces occurred during peak extension, and the maximum anteroposterior shear forces occurred during peak right lateral bending. Generally the shear forces were small in magnitude compared with compressive forces.

DISCUSSION

The specific goals of this study were to determine neck muscle forces and spinal loads that result from isometric efforts and to assess EMG activities of neck muscles during isometric efforts. For this purpose, an EMG-based model was formulated and an EMG experiment was performed. Hypothesis (i) is supported by the manifest existence of EMG activities in antagonistic muscles and a substantial variation in EMG activation patterns. The EMG-based model predicted antagonistic muscle forces and various muscle force distributions; thus hypothesis (ii) is supported. The EMG-based model predicted spinal compressive loads that were higher than previous reports that do not include antagonistic muscle forces; thus hypothesis (iii) is supported by this study.

EMG activities during isometric efforts. During MVC trials, most of the muscles showed relatively high

levels of EMG signals during rotation. However, it proved difficult to find a method that consistently produced maximum EMG signals at a certain location of the neck for all subjects. Therefore, various exertion strategies were employed to enhance the likelihood that the maximal EMG amplitude was obtained. During MVC trials, each subject was asked to sustain maximum effort for 1 s after 2 s of development. Fatigue was not considered a factor during the MVC efforts because of the brief duration of each contraction effort. This was demonstrated by the moments of the second or the third trials that were usually similar to or sometimes greater than those of the first trials were.

Observation of high levels of EMG activities as a percentage of MVC during maximum isometric rotation efforts is consistent with the results of Moroney et al. (16). The high levels of EMG activities of cervical muscles in rotation may indicate that a primary role of neck musculature is to provide rotation. This is in contrast to the reported EMG activities of lumbar muscles (14) where relatively high levels in bending and low levels in rotation suggested that bending is the primary role of lumbar musculature and rotation is secondary. These roles are confirmed by the orientation of the articular facets, restricting lumbar rotation, and allowing cervical rotation.

In the trapezius, it appeared that the starting position of rotation efforts affected the relative EMG level. A $+30^{\circ}$ prerotated starting position tended to increase the EMG level, and a -30° prerotated starting position tended to decrease the EMG level. This suggests that the starting position of rotation, and hence the muscle or sarcomere length, is related to the capability of muscle to contract. These high EMG activities are consistent with the muscle fiber directions of agonists on one side, which produce rotation, and the lower activity levels of their antagonistic

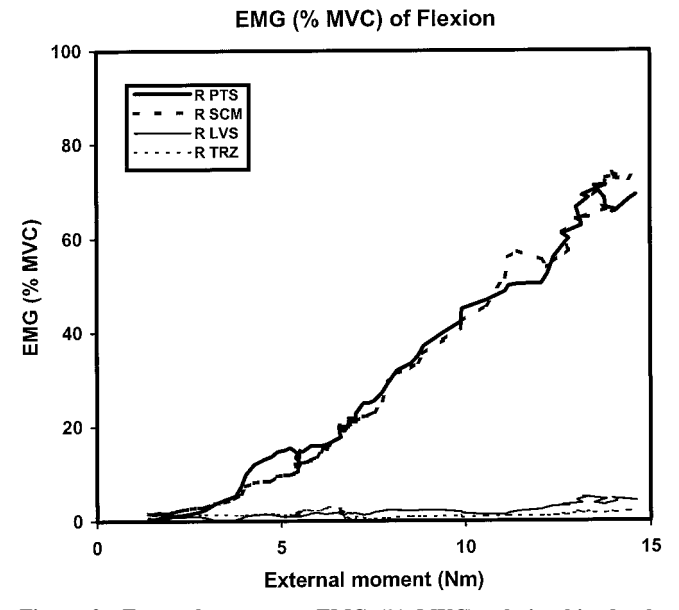


Figure 2—External moments—EMG (% MVC) relationship developed in attempted flexion (right side: subject 3). R PTS, right platysma; R SCM, right sternocleidomastoid; R LVS, right levator scapulae; R TRZ, right trapezius.

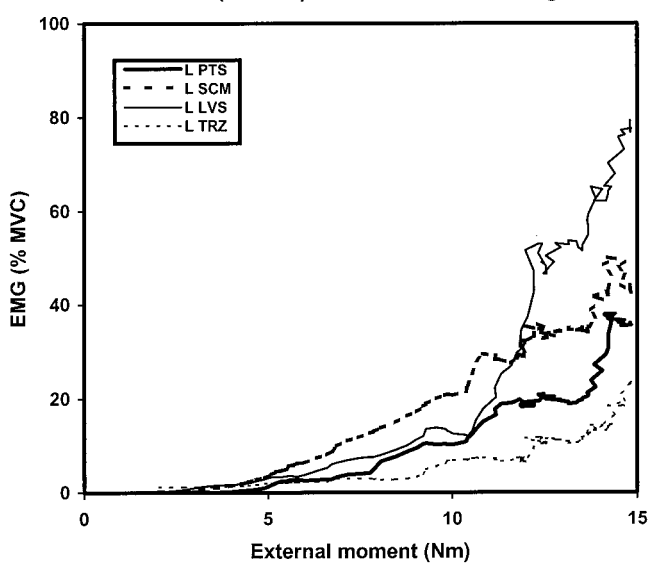


Figure 3—External moments—EMG (% MVC) relationship developed in attempted left lateral bending (left side: subject 3). L PTS, left platysma; L SCM, left sternocleidomastoid; L LVS, left levator scapulae; L TRZ, left trapezius.

counterparts. The high levels of EMG activities at the anterior and anterolateral electrodes on the side opposite the direction of attempted rotation are consistent with the observation of Moroney et al. (16).

The cutoff frequency of the low pass filter (3 Hz) was selected based on the following: The frequency responses of the rectus femoris was reported to be between 1.0 and 2.8 Hz during walking (17) and approximately 3 Hz in the first dorsal interosseous (15). McGill (13) reported that the 3 Hz

TABLE 4. Mean muscle forces predicted by EMG-based model during peak attempted moments, averaged across subjects, with SD in parentheses.

		Predicted Muscle Forces (N)			
Muscle Equivalents	Extension	Flexion	L Lat Bend	R Lat Bend	
L platysma	2 (1)	45 (16)	24 (8)	16 (8)	
R platysma	2 (1)	44 (16)	15 (7)	20 (8)	
L infrahyoid	5 (3)	145 (50)	76 (25)	50 (27)	
R infrahyoid	6 (4)	140 (52)	49 (24)	63 (27)	
L sternocleidomastoid	16 (6)	292 (145)	174 (45)	72 (48)	
R sternocleidomastoid	22 (12)	302 (89)	58 (41)	154 (42)	
L longus colli and cerv	3 (1)	53 (27)	32 (8)	13 (9)	
R longus colli and cerv	4 (2)	55 (16)	11 (7)	28 (8)	
L scalene anterior	4 (2)	73 (36)	43 (11)	18 (12)	
R scalene anterior	6 (3)	75 (22)	15 (10)	38 (10)	
L scalene medius	46 (19)	29 (24)	44 (22)	6 (4)	
R scalene medius	52 (14)	34 (13)	15 (9)	38 (16)	
L longissimus cerv	34 (12)	19 (15)	29 (14)	4 (3)	
R longissimus cerv	30 (9)	22 (9)	10 (5)	24 (10)	
L levator scapulae	126 (54)	83 (68)	128 (64)	17 (12)	
R levator scapulae	129 (40)	99 (38)	43 (25)	109 (45)	
L multifidus	49 (9)	10 (6)	29 (11)	10 (3)	
R multifidus	55 (13)	11 (5)	8 (6)	28 (8)	
L semispinalis cerv	89 (21)	23 (14)	67 (25)	22 (7)	
R semispinalis cerv	90 (29)	26 (11)	18 (12)	64 (19)	
L semispinalis cap	127 (28)	30 (19)	88 (33)	29 (9)	
R semispinalis cap	135 (39)	34 (15)	23 (17)	84 (25)	
L splenius cervicis	25 (7)	10 (7)	17 (8)	3 (1)	
R splenius cervicis	27 (5)	13 (5)	6 (3)	14 (6)	
L splenius capitis	56 (13)	14 (9)	42 (16)	14 (4)	
R splenius capitis	55 (19)	17 (7)	11 (8)	41 (12)	
L trapezius	68 (16)	38 (16)	51 (19)	17 (5)	
R trapezius	65 (22)	42 (18)	13 (10)	49 (15)	

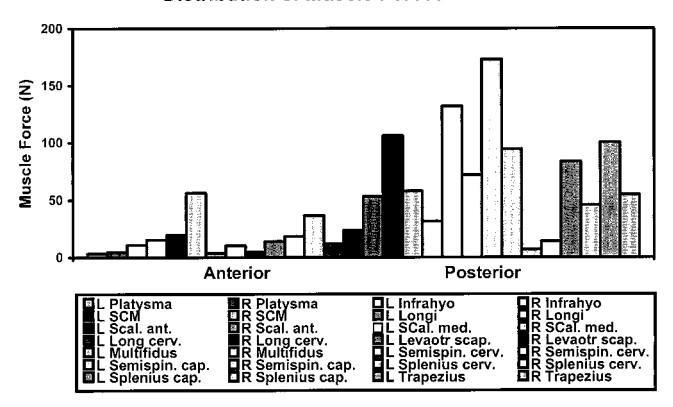


Figure 4—Example of muscle force distribution pattern during attempted peak extension of subject 5 (29.1 Nm). The EMG-based model shows antagonistic muscle forces. Each bar represents muscle force prediction.

cutoff in measuring dynamic lumbar spine muscle contractions produced an impulse of 53 ms, which is compatible with the 30–90 ms contraction times for a variety of muscles (1). Generally, when the contractions change quasi-statically, as in many isometric experiments, the low pass filter cutoff frequency can be lower, even to 1 Hz (7).

Model calculated muscle forces and spinal **loads.** The predicted muscle forces were dramatically different from those previously reported by the optimization method (16). The EMG-based model showed activation of all muscles including antagonistic co-contractions (Table 4; Figs. 4 through 6). The EMG-based approach also accommodated the variation of muscle force distribution patterns (Fig. 7). Prediction of both muscle forces and muscle force distribution patterns are needed to understand the mechanisms of muscle recruitment strategies. The muscle force distribution patterns are especially critical when evaluating the spine of an individual (2). The optimization approach, inherently, is not sensitive to the individual differences in the way people recruit their muscles when performing tasks. It satisfies three moment equilibrium constraints exactly and reaches the same muscle force distribution patterns for

Distribution of Muscle Forces in Flexion

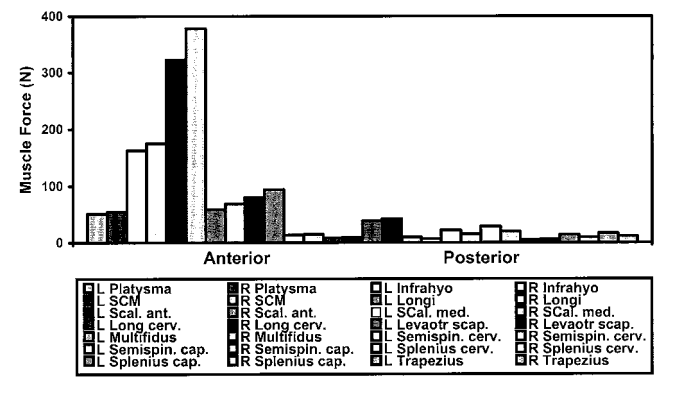


Figure 5—Example of muscle force distribution pattern during attempted peak flexion of subject 1 (13.6 Nm). The EMG-based model shows antagonistic muscle forces. Each bar represents muscle force prediction.

Distribution of Muscle Forces in Left Lateral Bending

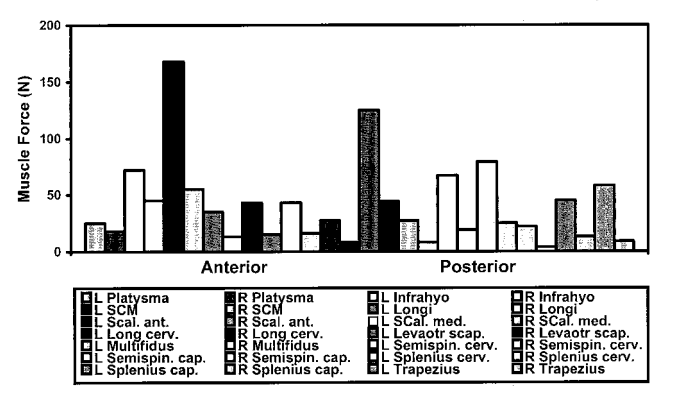


Figure 6—Example of muscle force distribution pattern during attempted peak left lateral bending of subject 3 (15.1 Nm). The EMG-based model shows antagonistic muscle forces. Each bar represents muscle force prediction.

every individual. Individuals do, however, alter their patterns of force distribution among the various muscles when performing repetitive task (18).

The compressive loads calculated in this study were higher than previously indicated (16) by approximately 11% in extension, 78% in flexion, and 15% in left lateral bending. The large discrepancies in joint compressive force reflect differences in the predictions of the amount of antagonistic co-contractions (Table 5). The variability in the results of the spinal loads, as expressed by the standard deviations (Table 5), was greater in the EMG-based approach than in the optimization approach. Generally, the resultant spinal compressive force indicates the extent of muscle co-contraction predicted by the model, and the variability reflects largely the individual difference in the muscle force distribution patterns (2).

Variation of Muscle Force Distribution Patterns

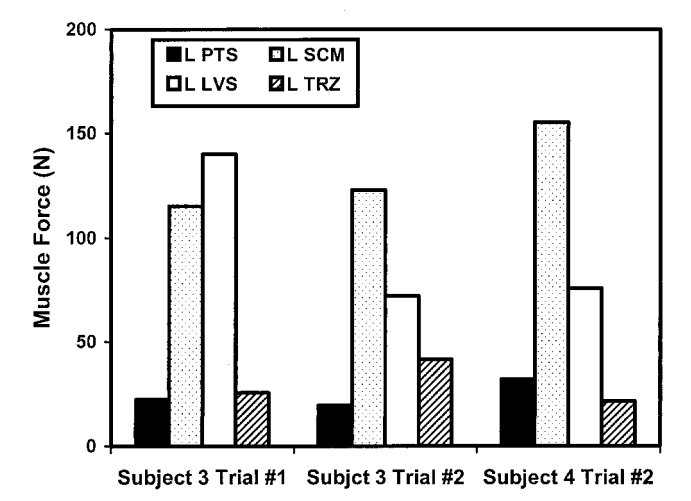


Figure 7—Example of different muscle force distribution patterns between subjects and between trials of the same subject among selected agonistic muscles. The model predicted muscle forces for 16 Nm of moment in attempted left lateral bending. L PTS, left platysma; L SCM, left sternocleidomastoid; L LVS, left levator scapulae; L TRZ, left trapezius.

TABLE 5. Mean spinal loads (lateral shear, anteroposterior shear, and compressive force) from EMG-based model during peak attempted moments, averaged across trials and subjects (SD in parentheses).

Exercises	Shear Lat.	Shear a-p	Compression
Extension	-1 (30)	-182 (28)	1372 (140)
Flexion	-28(24)	-162 (110)	1654 (308)
Left Lat. Bend	-77(36)	-74(32)	956 (169)
Right Lat. Bend	89 (39)	-98 (62)	1065 (207)

The effects of antagonistic muscle coactivation on lumbar spine stability and lumbar spine compression were estimated by using biomechanical lumbar spine models (3,6,26). Cholewicki et al. (3) examined the coactivation of trunk flexor and extensor muscles. Their study demonstrated that coactivation increased with added mass to the torso, and the coactivation was thought to enhance mechanical stability of the lumbar spine. Gardner-Morse and Stokes (6) estimated the effects of antagonistic abdominal coactivation by calculating the muscle stresses, the maximum compressive loading on the lumbar spine, and the critical value of muscle stiffness parameter. They reported that antagonistic abdominal coactivation increased stability of the spine at the cost of a small increase in maximum spinal compression. Thelen et al. (26) suggested that substantial contractions of lumbar muscles, especially during asymmetric exertions, increase stability at the L3-L4 level. Our computed results predicting antagonistic co-contractions and higher maximal compressive loads also suggest that antagonistic co-contractions provide stability to the human cervical spine around its neutral posture by stiffening the joints.

Maiman et al. (10) tested whole cervical spinal columns (skull-T3) for failure using compressive loads applied at the vertex. They applied compressive loads 2 cm posterior and 1 cm anterior to the vertex to simulate flexion and extension. They reported average axial loads at failure as 3567 N with no preflexion and 1823 N with preflexion. Shea et al. (23) reported the strength of the lower cervical spine (C5-T1) as 2158 N in compressive force. Considering these reports on spinal strength in compression, all of the maximal mean C4/5 joint compression force predicted from the model, 1654 N, is well below the spinal strength and hence does not violate physiologic constraints. The spinal loads calculated in this study are, however, in a range that could possibly cause tissue damage at prefailure loads. It must be also borne in mind that tests herein were done on young healthy males whereas most ex vivo testing is on older spines with less bone density and more structural compromise. In addition, ex vivo testing does not accurately simulate boundary conditions, muscle loading, etc.

Limitations. The most significant limitation of the experiment resulted from measuring EMG activity with surface electrodes. As such they could have been affected by cross-talk from signals of different muscles. Vink et al. (28) quantified cross-talk between electrodes by using 12 pairs of bipolar surface electrodes over the erector spine group during isometric contractions. They reported that the absolute maximum in the correlation coefficient was less than 0.3 when electrode pairs were placed more than 30 mm apart. They concluded that even at a distance of 30 mm, EMG

signals are specific and selectively record localized muscle activity in the erector spinae. In this study the distance between the electrode pairs was greater than 30 mm to minimize cross-talk between electrodes during exertions. Even though electrode pairs were placed more than 30 mm apart, there still may have been some EMG cross-talk from underlying muscles. This would explain why the EMG behaviors for the more anterior muscles (sparse muscle area) were closer to linear than for the more posterior (dense muscle area). EMG signal cross-talk would overpredict the muscle forces of less active muscles and underpredict the net moments. This would increase the estimated co-contraction, and, consequently, increase the estimated spinal compressive force.

Another possible limitation is that no distinctions about the mechanical functions of different muscles were made in spite of the functional differentiation in the muscles. By using surface electrodes, grouping of the muscles was inevitable. This forces an assumption that the muscles of the same group are the same in their EMG (% MVC) activities and functions. There are insufficient data to separate the detailed neural activation and functions of muscles within a group. In addition, the relationship between EMG activity of a muscle and its force is limited because this relationship was based upon eight regional EMG activities and a net moment from all agonist and antagonist muscles. Within these limitations, the EMG activity makes it possible to estimate the contribution of a specific muscle to a specific moment (14).

The concept that the muscle force is proportional to cross-sectional area of the muscle should be considered carefully. The cross-section was made perpendicular to the superior axis. But, in some muscles the directions of muscle fibers are not parallel to the superior axis. One must depend on anatomical accuracy to satisfy the moment equilibrium requirements about all three joint axes simultaneously (13). Individualized anatomic data would make the results more accurate and reliable. Lacking these data, linear geometric scaling of the cross-sectional anatomical data was used to estimate the individual anatomical data.

Validation of the model is still problematic because there is no direct way to measure the muscle and spinal forces. The correlation of predicted muscle forces with EMG amplitudes is usually used as evidence of model validity, particularly for optimization models. Since the EMG-based model uses the EMG amplitudes as its model-input values, the EMG-based model has inherent physiological validity. Another way to estimate the accuracy of the model is to calculate the errors in the external moments predicted by the model. In this study, the model showed the largest RMS

REFERENCES

- BUTCHTHAL, F., and H. SCHMALBRUCH. Contraction times and fibre types in intact human muscle. Acta Physiol. Scand. 79:435–452, 1970.
- CHOLEWICKI, J., and S. M. McGill. EMG assisted optimization: hybrid approach for estimating muscle forces in an indeterminate biomechanical model. *J. Biomech.* 27:1287–1289, 1994.

errors during attempted lateral bending in bending moments about all three orthogonal axes. During attempted extension or flexion, the moment about the anteroposterior axis is well balanced because of the laterally symmetric geometry of the neck musculature. During attempted lateral bending, however, the muscles on the side opposite the restraint rope are activated mostly to increase the resisting force. These muscles are not symmetric, with the anterior muscles being sparse compared with the posterior muscles. Hence, the anterior muscles on the same side as the restraint were activated to balance an induced moment about the lateral axis. This nonsymmetric geometry anterior versus posterior caused more errors in predicted moments about a lateral axis during lateral bending.

In this study age and gender effects were not considered. The maximum muscle force generated per unit of cross-sectional area (physiologic muscle strength) might need to vary according to age and gender. We examined isometric, static loading of the cervical spine and only one posture (neutral and upright). In dynamic loading conditions, the effects of muscle length change and the rate of muscle length change should be considered. A more extensive study with varying postures would be helpful to expand the biomechanical knowledge of the cervical spine.

CONCLUSIONS

This study suggests that higher (approximately 11% in extension, 78% in flexion, and 15% in left lateral bending) levels of C4/5 cervical spine loads are possible at maximum effort than previously reported by an optimization model (16) which does not include antagonistic co-contractions. The EMG-based model estimated a substantial variation of muscle force distribution patterns that corresponded to various EMG activation patterns. EMG-based method used in this study provides additional information about cervical spine loading that may be useful for surgical and rehabilitative considerations. Higher levels of physiological loads in the neck, as indicated in this study for voluntary contractions, must be considered possible during physical therapy.

The authors thank Dr. Kreg Gruben and Dr. Barbara Loitz-Ramage for their help in the experiment and their helpful suggestions.

This project was funded in part by a grant from University Surgical Associates through the University of Wisconsin Foundation.

Current address for H. Choi is Department of Physiology, Northwestern University, 303 E. Chicago Ave., Chicago, IL 60611.

Address for correspondence: Ray Vanderby Jr., Ph.D., University of Wisconsin, Division of Orthopedic Surgery, G5/330 Clinical Science Center, 600 Highland Avenue, Madison, WI 53792-3228. E-mail: vanderby@surgery.wisc.edu.

- CHOLEWICKI, J., M. M. PANJABI, and A. KHACHATRYAN. Stabilizing function of trunk flexor-extensor muscles around a neutral spine posture. Spine 22:2207–2212, 1997.
- 4. Cholewicki, J., S. M. McGill, and R. W. Norman. Comparison of muscle forces and joint load from an optimization and EMG

- assisted lumbar spine model: towards development of hybrid approach. *J. Biomech.* 28:321–331, 1995.
- CLAUSER, C. E., J. T. McConville, and J. W. Young. Weight, volume, and center of mass of segments of the human body. Wright-Patterson Air Force Base, OH: AMRL-TR-69-70, 1969, pp. 1-101.
- GARDNER-MORSE, M. G., and I. A. STOKES. The effects of abdominal muscle coactivation on lumbar spine stability. *Spine* 23:86– 92, 1998.
- Hof, A. L. EMG and muscle force: an introduction. Hum. Mov. Sci. 3:119–153, 1984.
- Hughes, R. E., J. C. Bean, and D. B. Chaffin. Evaluating the effect of co-contraction in optimization models. *J. Biomech.* 28:875– 878, 1995.
- LADIN, Z., K. R. MURTHY, and C. J. DELUCA. Mechanical recruitment of low back muscles. Spine 14:927–938, 1989.
- MAIMAN, D. J., A. SNACES, J. B. MYKLEBUST, et al. Compression injuries of the cervical spine: a biomechanical analysis. *Neuro-surgery* 13:254–260, 1983.
- MARRAS, W. S. Predictions of forces acting upon the lumbar spine under isometric and isokinetic conditions: a model experiment comparison. *Int. J. Ind. Ergonomics* 3:19–27, 1988.
- McGill, S. M., and R. W. Norman. Partitioning of the L4/L5 dynamic moment into disc, ligamentous, and muscular component during lifting. Spine 11:666–678, 1986.
- 13. McGill, S. M. A myoelectrically based dynamic three-dimensional model to predict loads on lumbar spine tissues during lateral bending. *J. Biomech.* 25:395–414, 1992.
- McGill, S. M. Electromyographic activity of the abdominal and low back musculature during the generation of isometric dynamic axial trunk torque: implications for lumbar mechanics. *J. Orthop. Res.* 9:91–103, 1991.
- MILNER-BROWN, H. S., R. B. STEIN, and R. YEMM. The contractile properties of human motor units during voluntary isometric contractions. *J. Physiol.* 228:285–306, 1973.
- MORONEY, S. P., A. B. SCHULTZ, and J. A. A. MILLER. Analysis and measurement of neck loads. J. Orthop. Res. 6:713–720, 1988.
- OLNEY, S. J., and D. A. WINTER. Predictions of knee and ankle moments of force in walking from EMG and kinematic data. *J. Biomech.* 18:9–20, 1985.

- POTVIN, J. R., and R. W. NORMAN. Quantification of erector spinae muscle fatigue during prolonged, dynamic lifting tasks. *Eur. J. Appl. Physiol. Occup. Physiol.* 67:554–562, 1993.
- SCHULTZ, A. B., G. B. J. ANDERSSON, K. HADERSPECK, R. ORTEN-GREN, M. NORDIN, and R. BJORK. Analysis and measurements of lumbar trunk loads in tasks involving bends and twists. *J. Bio*mech. 15:669–675, 1982.
- SCHULTZ, A. B., G. B. J. ANDERSSON, R. ORTENGREN, K. HADERSPECK, and A. NACHEMSON. Loads on the lumbar spine: validation of a biomechanical analysis by measurements of intradiscal pressure and myoelectric signals. *J. Bone Joint Surg.* 64:713–720, 1982.
- SCHULTZ A. B., G. B. J. ANDERSSON, R. ORTENGREN, R. BJORK, and M. NORDIN. Analysis and quantitative myoelectric measurements of loads on the lumbar spine when holding weights in standing postures. Spine 7:390–397, 1982.
- SCHULTZ, A. B., R. CROMWELL, D. WARWICK, and G. B. J. ANDERS-SON. Lumbar trunk muscle use in standing isometric heavy exertions. *J. Orthop. Res.* 5:320–326, 1987.
- SHEA, M., W. T. EDWARDS, A. A. WHITE, and W. C. HAYES. Variations of stiffness and strength along the human cervical spine. *J. Biomech.* 24:95–107, 1991.
- SLUCKY, A. V., and F. J. EISMONT. Treatment of acute injury of cervical spine. J. Bone Joint Surg. 76-A:1882–1896, 1994.
- STOKES, I. A. F., S. RUSH, M. MOFFROID, G. B. JOHNSON, and L. D. HAUGH. Trunk extensor EMG-torque relationship. *Spine* 12:770–776, 1987.
- THELEN, D. G., A. B. SCHULTZ, and J. A. ASHTON-MILLER. Cocontraction of lumbar muscles during the development of timevarying triaxial moments. *J. Orthop. Res.* 13:390–398, 1995.
- TORG, J. S., H. PAVLOV, M. J. O'NEILL, C. E. III NICHOLS, and B. SENNETT. The axial load teardrop fracture: a biomechanical, clinical, and roentgenographic analysis. *Am. J. Sports Med.* 19:355–364, 1991.
- VINK, P., H. A. M. DAANEN, and A. J. VERBOUT. Specificity of surface-EMG on the intrinsic lumbar back muscles. *Hum. Mov.* Sci. 8:67–78, 1989.
- VINK, P., E. A. VAN DER VELDE, and A. J. VERBOUT. A functional subdivision of the lumbar extensor musculature. *Electromyogr. Clin. Neurophysiol.* 27:517–525, 1987.